

# Geminal Dicationic Ionothermal Synthesis of One Three-Dimensional Luminescent Strontium(II) Coordination Polymer Based on 1,4-Naphthalenedicarboxylate Acid<sup>1</sup>

W. J. Zhu<sup>a</sup>, Z. J. Qin<sup>a</sup>, Y. Bai<sup>a</sup>, <sup>\*,</sup> and D. B. Dang<sup>a</sup>, <sup>\*\*</sup>

<sup>a</sup>Henan Key Laboratory of Polyoxometalate Chemistry, Institute of Molecular and Crystal Engineering, College of Chemistry and Chemical Engineering, Henan University, Kaifeng, 475004 P.R. China

<sup>\*</sup>e-mail: baiyan@henu.edu.cn

<sup>\*\*</sup>e-mail: dangdb@henu.edu.cn

Received September 9, 2017

**Abstract**—One three-dimensional Sr(II) coordination polymer  $[C_6(MIm)_2][Sr_3(1,4-NDC)_4]$  (**I**) ( $C_6(MIm)_2$  = 1,3-bis(3-methylimidazolium-1-yl)hexyl, 1,4-H<sub>2</sub>NDC = 1,4-naphthalenedicarboxylate acid) has been synthesized using an ionothermal method and structurally characterized by IR spectroscopy, UV-Vis spectroscopy, XRPD, and X-ray single-crystal structure analysis (CIF file CCDC 1033958). Two types of strontium centers are bridged by two coordination modes of 1,4-H<sub>2</sub>NDC ligands to form a Sr(II) chain. Each Sr(II) chain is cross-connected to four other chains to generate a 3D coordination polymer, in which  $C_6(MIm)_2^{2+}$  cations as charge balancing species are filled in the channels of the anionic framework. The polymeric solid of **I** exhibits strong luminescent emission at room temperature.

**Keywords:** ionothermal synthesis, strontium, coordination polymer, luminescent properties

**DOI:** 10.1134/S1070328418070096

## INTRODUCTION

The field of coordination polymers (CPs) has been growing tremendously over recent years because of their various intriguing architectures and excellent properties as well as potential applications in many fields, such as adsorption, separation, purification and catalysis [1–4]. One of the remarkable synthesis methods of CPs developing recently is ionothermal synthesis [5]. With the unusual properties such as good thermal and chemical stability, extended hydrogen bonding and template providers, ionic liquids (ILs) can act as “supersolvents” to provide excellent reaction environment that can make specific changes in the self-assembly process at the molecular level and give rise to generating solid materials with fantastic structural motifs and outstanding properties [6–8]. Although quite a lot of examples of ILs participating in the synthesis of CPs have been reported, most of them are on monocationic ionic liquids (MILs) such as imidazole-containing MILs [9–13]. In contrast to MILs with monovalent cations, geminal dicationic ionic liquids (DILs), possessing higher densities and viscosities, greater thermal stabilities and wider liquid ranges, could afford a peculiar environment for the synthesis reaction. Especially, the higher electric

charge density could make them the better structure-director to get unprecedented structures. In 2014, we have explored the ionothermal synthesis of  $Ni(Ac)_2$ –1,4-H<sub>2</sub>NDC system using four geminal 1,3-bis(3-methylimidazolium-1-yl)alkyl bromide DILs as solvents for the first time [14]. Herein, as a part of our continuing investigations on the alkaline earth-organic frameworks [9], we report ionothermal synthesis and structural characterization of an interesting 3D coordination polymer  $[C_6(MIm)_2][Sr_3(1,4-NDC)_4]$  (**I**) displaying strong fluorescent emission using 1,3-bis(3-methylimidazolium-1-yl)hexyl bromide as solvent.

## EXPERIMENTAL

**Materials and methods.** All chemicals employed in this study were analytically pure, from commercial sources and used without further purification. Ionic liquid  $C_6(MIm)_2Br_2$ , 1,3-bis(3-methylimidazolium-1-yl)hexyl bromide, was prepared according to the literature method [15, 16]. Elemental analyses (C, H, and N) were performed on a Perkin-Elmer 240C analytical instrument. IR (KBr pellets) spectra were recorded using a Nicolet 170 SXFT-IR spectrophotometer in the 400–4000  $cm^{-1}$  range. The UV-Vis

<sup>1</sup> The article is published in the original.

**Table 1.** Crystallographic data and structure refinement information for **I**

Parameter	Value
Diffractometer	Bruker Smart APEX II CCD
Temperature, K	296(2)
Crystal system	Monoclinic
Space group	$P2_1/n$
$a$ , Å	12.8639(8)
$b$ , Å	13.9067(8)
$c$ , Å	16.0119(10)
$\beta$ , deg	99.757 (1)
$V$ , Å <sup>3</sup>	2823.0 (3)
$Z$	2
$\rho_{\text{calcd}}$ , g cm <sup>-3</sup>	1.609
$\mu$ , mm <sup>-1</sup>	2.901
$F(000)$	1380
$\theta$ Range for data collection, deg	1.88–25.00
Scan mode	$\omega$
Number of unique reflections ( $N_1$ )	4972 ( $R_{\text{int}} = 0.0594$ )
Number of reflections with $I > 2\sigma(I)$ ( $N_2$ )	2894
Number of parameters refined	385
GOOF ( $F^2$ )	1.042
$R_1$ for $N_2$	0.0699
$wR_2$ for $N_1$	0.1850
$\Delta\rho_{\text{max}}/\Delta\rho_{\text{min}}$ , e Å <sup>-3</sup>	1.422/–0.887

spectra were obtained on a Shimazu UV-250 spectrometer in the range of 800–190 nm in the solid state. X-ray powder diffraction patterns (XRPD) were recorded on a D/max- $\gamma$  A rotating anode X-ray diffractometer with Cu sealed tube ( $\lambda = 1.54178$  Å). The luminescent spectra were performed on a Hitachi F-7000 fluorescence spectrophotometer.

**Synthesis of complex I** was carried out by ionothermal method. A mixture of Sr(NO<sub>3</sub>)<sub>2</sub> (0.284 g, 1.0 mmol), 1,4-H<sub>2</sub>NDC (0.216 g, 1.0 mmol) and NaOH (0.080 g, 2.0 mmol) in C<sub>6</sub>(MIm)<sub>2</sub>Br<sub>2</sub> (1.0 g) was sealed into a 25 mL Teflon lined stainless-steel container and heated at 180°C for 120 h. Then the autoclave was cooled to room temperature and the red crystals were isolated and washed with ethanol. The total yield was 54% based on 1,4-H<sub>2</sub>NDC.

For C<sub>62</sub>H<sub>48</sub>N<sub>4</sub>O<sub>16</sub>Sr<sub>3</sub> ( $M = 1367.90$ )

Anal. calcd., %	C, 54.44	H, 3.54	N, 4.09
Found, %	C, 54.67	H, 3.42	N, 3.95

IR (KBr;  $\nu$ , cm<sup>-1</sup>): 3341 m, 1649 m, 1553 s, 1462 m, 1419 s, 1371 s, 1262 m, 1211 w, 1168 w, 883 w, 842 m, 824 w, 797 m, 619 m, 586 m, 454 w, 434 w.

**X-ray crystallography.** A suitable crystal of size 0.34 × 0.21 × 0.18 mm was chosen for the crystallographic study and mounted on a Bruker Smart APEX II CCD diffractometer. All diffraction measurements were performed at room temperature using graphite-monochromatized MoK $\alpha$  radiation ( $\lambda = 0.71073$  Å). The structure was solved by direct methods and refined on  $F^2$  by using full-matrix least-squares methods with the SHELXL-97 program [17, 18]. Space group, lattice parameters and other relevant information are listed in Table 1 and selected bond lengths and angles are given in Table 2.

Supplementary material for structure **I** has been deposited with the Cambridge Crystallographic Data Centre (no. 1033958; [www.ccdc.cam.ac.uk/data\\_request/cif](http://www.ccdc.cam.ac.uk/data_request/cif)).

## RESULTS AND DISCUSSION

The IR spectrum of polymer **I** exhibits the characteristic bands of the carboxy group coordinating to the metallic ion. The strong absorption band at 1553 cm<sup>-1</sup> shows the characteristic stretching frequency of  $\nu_{\text{as}}(\text{CO}_2)$ , and the bands at 1419 and 1371 cm<sup>-1</sup> are

**Table 2.** Selected bond lengths (Å) and bond angles (deg) of **I**\*

Bond	<i>d</i> , Å	Bond	<i>d</i> , Å
Sr(1)–O(1)	2.490(5)	Sr(1)–O(5)	2.575(6)
Sr(1)–O(4F)	2.499(5)	Sr(2)–O(3F)	2.412(7)
Sr(2)–O(5B)	2.748(5)	Sr(2)–O(2)	2.483(6)
Sr(2)–O(6B)	2.447(8)	Sr(2)–O(7D)	2.617(8)
Sr(2)–O(8C)	2.577(8)	Sr(2)–O(8D)	2.677(8)
Angle	$\omega$ , deg	Angle	$\omega$ , deg
O(1)Sr(1)O(4F)	91.5(2)	O(1)Sr(1)O(4G)	88.5(2)
O(4G)Sr(1)O(5)	94.0(2)	O(1)Sr(1)O(5)	92.7(2)
O(1)Sr(1)O(5B)	87.3(2)	O(2)Sr(2)O(5B)	86.7(2)
O(4F)Sr(1)O(5)	86.0(2)	O(2)Sr(2)O(8C)	154.1(3)
O(2)Sr(2)O(8D)	92.1(2)	O(2)Sr(2)O(7D)	78.2(2)
O(3F)Sr(2)O(5B)	84.0(2)	O(3F)Sr(2)O(6B)	120.6(3)
O(3F)Sr(2)O(2)	80.8(2)	O(3F)Sr(2)O(8C)	89.6(3)
O(3F)Sr(2)O(8D)	128.3(2)	O(3F)Sr(2)O(7D)	158.5(3)
O(6B)Sr(2)O(5B)	49.9(2)	O(6B)Sr(2)O(7D)	75.5(3)
O(6B)Sr(2)O(2)	123.1(3)	O(6B)Sr(2)O(8D)	106.1(3)
O(7D)Sr(2)O(5B)	99.1(2)	O(6B)Sr(2)O(8C)	82.5(3)
O(8C)Sr(2)O(5B)	116.3(2)	O(8D)Sr(2)O(5B)	147.1(2)
O(7D)Sr(2)O(8D)	48.7(2)	O(8C)Sr(2)O(8D)	75.1(2)
O(8C)Sr(2)O(7D)	107.6(3)		

\* Symmetry codes: (B)  $2 - x, 1 - y, -z$ ; (C)  $0.5 + x, 0.5 - y, -0.5 + z$ ; (D)  $2.5 - x, 0.5 + y, 0.5 - z$ ; (F)  $2.5 - x, -0.5 + y, 0.5 - z$ ; (G)  $-0.5 + x, 1.5 - y, -0.5 + z$ .

assigned as the  $\nu_s(\text{CO}_2)$  stretching frequency [9, 19]. The separation value of  $134 \text{ cm}^{-1}$  indicates that the carboxyl groups of 1,4-H<sub>2</sub>NDC have joined in different coordination modes, which agrees well with the date of the other relevant compounds [9, 20, 21]. These results were finally confirmed by X-ray crystallography.

The structure analysis by X-ray single crystal diffraction reveals that **I** exhibits a new crystalline 3D coordination polymer constructed through the coordination of deprotonated 1,4-NDC<sup>2-</sup> ligands and strontium(II) metal ions with  $[\text{C}_6(\text{MIm})_2]^{2+}$  cations as templates.

There are two crystallographically independent strontium(II) metal ions and each has a different coordination environment (Fig. 1). Sr(1) atom (in inversion center) is bound to six oxygen atoms O(1), O(1B), O(4F), O(4G), O(5) and O(5B) from six 1,4-NDC<sup>2-</sup> ligands to attain a distorted octahedral geometry. The Sr(1)–O distances are in the range of 2.490(5)–2.575(6) Å. The seven-coordinated Sr(2) ion adopts a capped trigonal prismatic coordination mode, which bonds to two oxygen atoms (O(2), O(3F)) of two  $\mu_2\text{-}\eta^1\text{:}\eta^1$  groups and five oxygen atoms (O(5B), O(6B), O(7D), O(8C) and O(8D)) of three  $\mu_2\text{-}\eta^2\text{:}\eta^1$  groups. O(7D) occupies the capped position with the Sr–O

distance of 2.617(8) Å. The rest of Sr(2)–O distances are in the range of 2.412(7)–2.748(5) Å.

In the asymmetric unit of **I**, two deprotonated 1,4-NDC<sup>2-</sup> ligands present two bridging modes,  $\mu_4\text{-}(\mu_2\text{-}\eta^1\text{:}\eta^1\text{-})(\mu_2\text{-}\eta^1\text{:}\eta^1)$  (NDC-1) and  $\mu_4\text{-}(\mu_2\text{-}\eta^2\text{:}\eta^1\text{-})(\mu_2\text{-}\eta^2\text{:}\eta^1)$  (NDC-2), respectively (Fig. 2). The linkages of Sr(1) and Sr(2) are two  $\mu_2\text{-}\eta^1\text{:}\eta^1$  carboxyl groups of two NDC-1 and one  $\mu_2\text{-}\eta^2\text{:}\eta^1$  group of NDC-2, while the linkages of adjacent two Sr(2) are a pair of  $\mu_2\text{-}\eta^2\text{:}\eta^1$  groups of two NDC-2 (Fig. 3). The Sr···Sr distance is 4.36 Å for Sr(1)···Sr(2) and 4.17 Å for Sr(2)···Sr(2), respectively. Therefore, adjacent Sr atoms are linked by the above bridging coordination interactions to generate a  $[\text{Sr}(1)\cdots\text{Sr}(2)\cdots\text{Sr}(2)]_n$  chain running parallel to the *x* axis with Sr(1)···Sr(2)···Sr(2) angle of 172°. Each chain links to the neighboring four chains through NDC-1 and NDC-2 giving rise to a 3D anionic framework structure, in which there are two types of C–H···π interactions between two benzene rings of NDC-1 and NDC-2 with the C–H···π separations of 3.29, 3.03 Å and the C–H···π angles of 118.8°, 129.7°, respectively (Fig. 4).  $[\text{C}_6(\text{MIm})_2]^{2+}$  cations acting as extra charge balancing species occupy the channels of the anionic framework and have a great influence on structure in the solid state (Fig. 5). It is interesting to note that there are obvious face-to-face π–π interactions and C–H···π

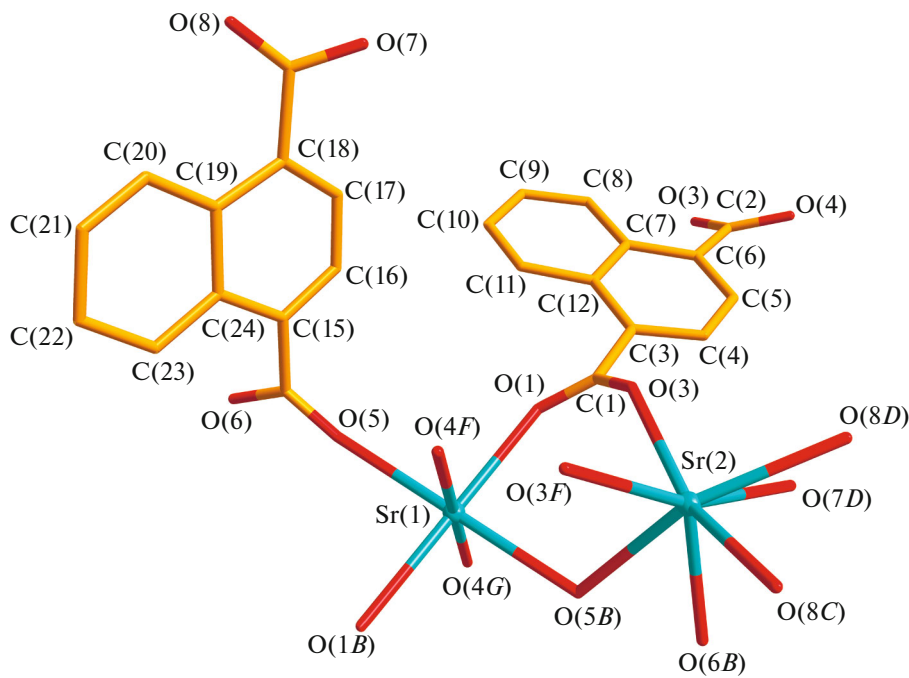


**Fig. 1.** A perspective view of **I** with the atom numbering scheme. All the H atoms are omitted for clarity. Symmetry codes: (B)  $2 - x, 1 - y, -z$ ; (C)  $0.5 + x, 0.5 - y, -0.5 + z$ ; (D)  $2.5 - x, 0.5 + y, 0.5 - z$ ; (F)  $2.5 - x, -0.5 + y, 0.5 - z$ ; (G)  $-0.5 + x, 1.5 - y, -0.5 + z$ .

interactions involving benzene rings of NDC-1 and imidazole rings of  $[C_6(MIm)_2]^{2+}$ . The  $\pi-\pi$  interactions are characterized by the centroid-centroid separation of 3.70 Å, the shortest interplanar atom–atom separation of 3.54 Å, and the dihedral angel of 12.0°, respectively. The C– $\pi$  separation is 3.86 Å and the C–H– $\pi$  angle is 73.5°. In addition, multiple hydrogen bonds can be

found in three-dimensional framework (Table 3). Apparently, the cooperativity of multiple interactions throughout the crystal plays an important role in stabilizing the solid structure.

To confirm the phase purity and to examine the crystallinity of bulk samples, XRPD measurement was performed for polymer **I**. The peak positions of simulated and experimental patterns are in good agreement with each other, demonstrating the phase purity of the products. The dissimilarities in intensity may be due to the variation in preferred orientation of the crystalline powder samples during collection of the experimental XRPD.

The UV-Vis absorption spectrum of polymer **I** in solid state has been measured in range of 190–700 nm at room temperature. As shown in Fig. 6a, the absorption edge of polymer **I** is around 700 nm. The obvious absorption peak at about 304 nm and a shoulder peak at 246 nm are observed, which are assigned to ligand-centered  $\pi-\pi^*$  charge transition from 1,4-H<sub>2</sub>NDC.

The band gap ( $E_g$ ) is a major factor determining the electrical conductivity of a solid and generally refers to the energy difference between the highest valence band and the lowest conduction band. To research the conductivity potential of polymer **I**, the  $E_g$  value is obtained as the intersection point between the energy axis and the line extrapolated from the linear portion of the absorption edge in a plot of Kubelka–Munk function  $F$  against energy  $E$ , in which  $F = (1 - R)^2/2R$

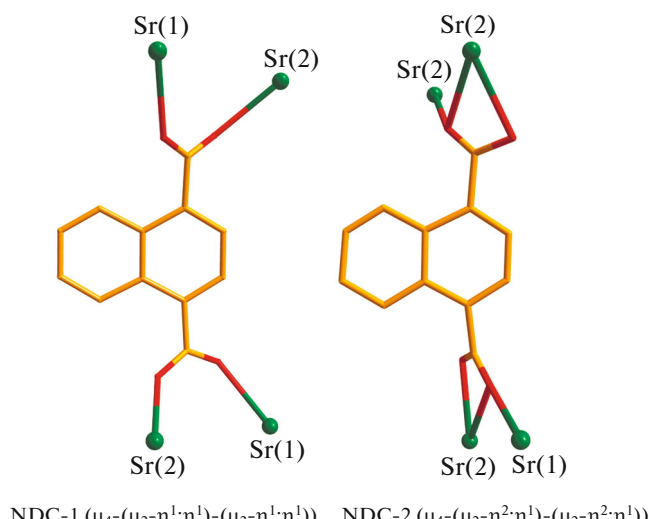


**Fig. 2.** Crystallographically established coordination modes of 1,4-NDC<sup>2-</sup> in **I**.

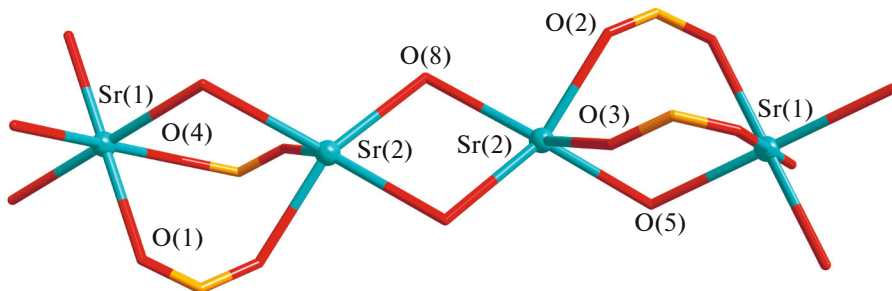


Fig. 3. Representation of Sr(II) chain in polymer I.

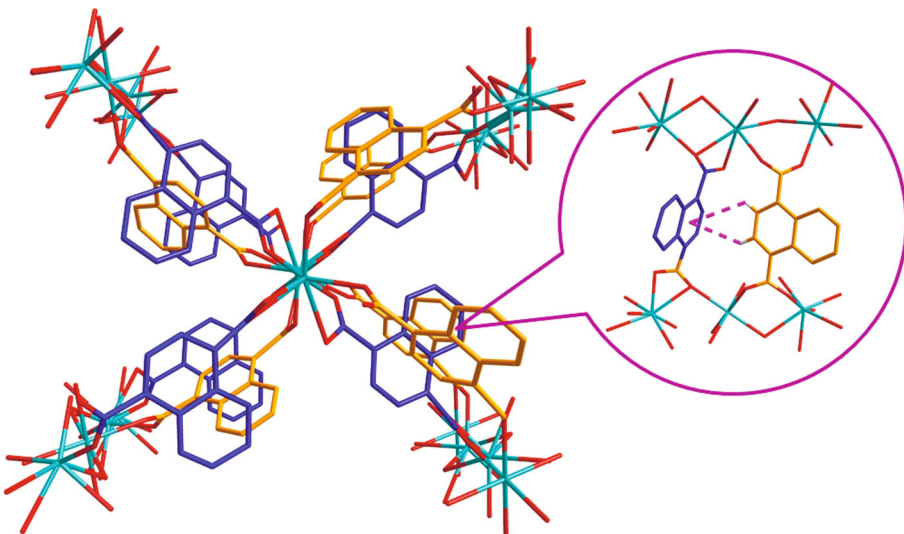


Fig. 4. The 3D structure of I and the C-H... $\pi$  interactions between two types of 1,4-NDC<sup>2-</sup>.

and  $R$  is the reflectance of an infinitely thick layer at a given wavelength. The  $F$  versus  $E$  plots is shown in Fig. 6b. The  $E_g$  value of polymer I can be assessed at 3.38 eV, which is very similar to that of zinc oxide (3.37 eV) at 300 K.

A strategy of the introduction of 1,4-naphthalenedicarboxylic acid as a photochemically active compound into coordination polymers is anticipated to obtain functional hybrid materials with excellent optical properties [22, 23]. Luminescent properties of polymer I have been investigated in the solid state at room temperature. As expected, the emission spectrum of I shows a strong emission band at 388 nm when excited at 345 nm, which is similar to that of  $(\text{EMIm})_4[\text{Sr}_{10}(1,4\text{-NDC})_{10}\text{Br}_4]$  at 377 nm (Fig. 7) [9]. The emission of I may be assigned to cooperativity of aromatic components  $\pi-\pi^*$  charge transition and oxygen to Sr(II) charge transfer transitions.

Thus, a new coordination polymer  $[\text{C}_6(\text{MIm})_2]\text{-}[\text{Sr}_3(1,4\text{-NDC})_4]$  (I) based on 1,4-naphthalenedicarboxylic acid has been ionothermally synthesized with an imidazolium-based geminal dicationic ionic liquid

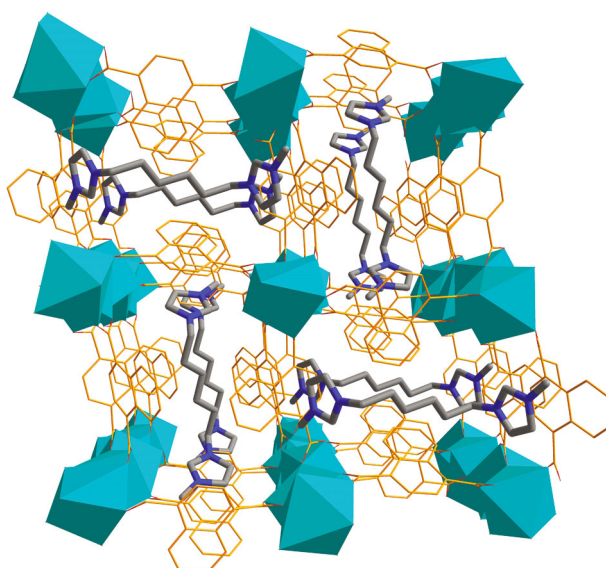
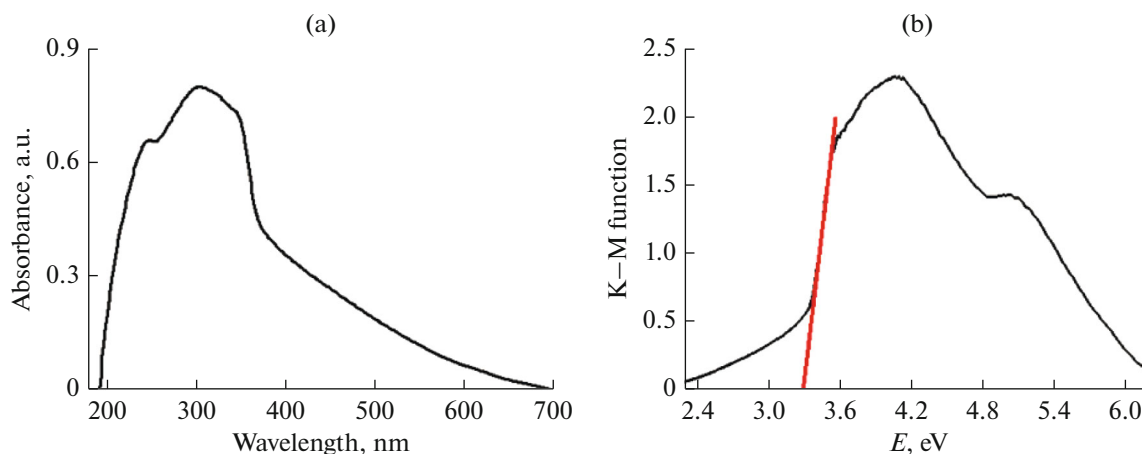
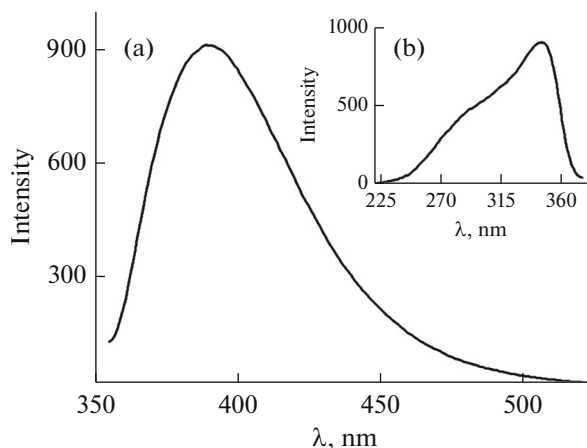


Fig. 5. The 3D framework of I containing  $[\text{C}_6(\text{MIm})_2]^{2+}$  cations (Sr, cyanic polyhedra). The hydrogen atoms have been omitted for clarity.

**Table 3.** Geometric parameters of hydrogen bonds for **I**

D—H···A	Distance, Å			Angle DHA, deg	Symmetry codes of atom A
	D—H	H···A	D···A		
C(4)—H(4A)···O(7)	0.93	2.59	3.502(11)	166	$5/2 - x, 1/2 + y, 1/2 - z$
C(8)—H(8A)···O(3)	0.93	2.30	2.868(10)	119	
C(11)—H(11A)···O(1)	0.93	2.44	2.989(9)	118	
C(17)—H(17A)···O(7)	0.93	2.41	2.736(14)	100	
C(20)—H(20A)···O(8)	0.93	2.32	2.944(17)	124	
C(25)—H(25A)···O(3)	0.96	2.60	3.387(13)	140	$5/2 - x, -1/2 + y, 1/2 - z$
C(26)—H(26A)···O(4)	0.93	2.33	3.190(10)	154	$5/2 - x, -1/2 + y, 1/2 - z$
C(27)—H(27A)···O(6)	0.93	2.53	3.339(14)	145	$1/2 + x, 1/2 - y, -1/2 + z$
C(28)—H(28A)···O(2)	0.93	2.52	3.416(12)	162	$-1/2 + x, 1/2 - y, -1/2 + z$

**Fig. 6.** The UV-Vis absorption spectrum of **I** in the solid state (a); diffuse reflectance UV-Vis spectrum of K-M function versus  $E$  (b).**Fig. 7.** The emission spectrum (a) ( $\lambda_{\text{ex}} = 345$  nm) and excitation spectrum (b) ( $\lambda_{\text{em}} = 388$  nm) of **I** in solid state at room temperature.

$\text{C}_6(\text{MIm})_2\text{Br}_2$  as solvent. The structure of **I** has been established by single-crystal X-ray diffraction analysis and exhibits a crystalline three-dimensional polymer constructed by the connection of Sr(II) and two bridging types of deprotonated 1,4-NDC<sup>2-</sup> ligands,  $\mu_4$ -( $\mu_2$ - $\eta^1$ : $\eta^1$ )-( $\mu_2$ - $\eta^1$ : $\eta^1$ ) and  $\mu_4$ -( $\mu_2$ - $\eta^2$ : $\eta^1$ )-( $\mu_2$ - $\eta^2$ : $\eta^1$ ), in which  $[\text{C}_6(\text{MIm})_2]^{2+}$  cations as structure templates and charge compensating groups enter the resulting framework. Band gap of 3.38 eV implies that polymer **I** is potential semiconductor. As expected, polymer **I** exhibits the obvious luminescence emission in the solid state due to the introduction of functional organic ligand. So ionothermal synthesis is an efficient way to the design and construction of functional coordination polymers. Further such studies are currently underway.

## ACKNOWLEDGMENTS

This work was supported by the National Natural Science Foundation of China (nos. 21471045, 21571049), the Foundation of Education Department of Henan Province of China (13A150045, 14A150022) and the Foundation of Students Innovative Experiment Program of Henan University.

## REFERENCES

1. Duan, J.G., Jin, W.Q., and Kitagawa, S., *Coord. Chem. Rev.*, 2017, vol. 48, p. 332.
2. Wang, C.H., Liu, X.L., Demir, N.K., et al., *Chem. Soc. Rev.*, 2016, vol. 45, p. 5107.
3. Vellingiri, K., Kumar, P., and Kim, K.H., *Nano. Res.*, 2016, vol. 9, p. 3181.
4. Gangu, K.K., Maddila, S., Mukkamala, S.B., et al., *Inorg. Chim. Acta*, 2016, vol. 61, p. 446.
5. Zhang, B.X., Zhang, J.L., and Han, B.X., *Chem.-Asian J.*, 2016, vol. 11, p. 2610.
6. Zhang, Z.H., Liu, B., Xu, L., et al., *Dalton Trans.*, 2015, vol. 44, p. 17980.
7. Mondal, S.S., Bhunia, A., Attallah, A.G., et al., *Chem.-Eur. J.*, 2016, vol. 22, p. 6905.
8. Li, L., Chen, S., Ning, Y.J., et al., *Russ. J. Coord. Chem.*, 2014, vol. 40, p. 904. doi 10.1134/S1070328414120082
9. Liu, S.S., Cheng, M., Li, B., et al., *J. Inorg. Organomet.*, 2015, vol. 25, p. 1103.
10. An, B., Wang, J.L., Bai, Y., et al., *Dalton Trans.*, 2015, vol. 44, p. 14666.
11. Liu, S.S., Zhou, R.M., Chen, S., et al., *Synth. React. Inorg., Met.-Org., Nano-Met. Chem.*, 2015, vol. 45, p. 112.
12. Chen, W.X., Bai, J.Q., Yu, Z.H., et al., *Chem. Commun.*, 2015, vol. 60, p. 4.
13. Liu, S.S., Zhou, R.M., Chen, S., et al., *Z. Naturforsch., B*, 2014, vol. 69, p. 864.
14. An, B., Bai, Y., Wang, J.L., et al., *Dalton Trans.*, 2014, vol. 43, p. 12828.
15. Zeng, Z., Phillips, B.S., Xiao, J.C., et al., *Chem. Mater.*, 2008, vol. 20, p. 2719.
16. Tadesse, H., Blake, A.J., Champness, N.R., et al., *CrystEngComm*, 2012, vol. 14, p. 4886.
17. Sheldrick, G.M., *Acta Crystallogr., Sect. A: Found. Crystallogr.*, 1990, vol. 46, p. 467.
18. Sheldrick, G.M., *Acta Crystallogr., Sect. A: Found. Crystallogr.*, 2008, vol. 64, p. 112.
19. Sun, D., Luo, G.G., Zhang, N., et al., *Polyhedron*, 2010, vol. 29, p. 1243.
20. Wu, Z.F., Hu, B., Feng, M.L., et al., *Inorg. Chem. Commun.*, 2011, vol. 14, p. 1132.
21. An, B., Zhou, R.M., Dang, D.B., et al., *Sectrochim. Acta, A*, 2014, vol. 122, p. 392.
22. Wei, J.J., Liu, Q.Y., Wang, Y.L., et al., *Inorg. Chem. Commun.*, 2012, vol. 15, p. 61.
23. Huang-Fu, Y.J., Chen, X.Y., Yang, W., et al., *Mater. Lett.*, 2015, vol. 155, p. 48.